Biogeochemistry (2005) 75: 83–107
DOI 10.1007/s10533-004-6320-z

River nutrient loads and catchment size

S.V. SMITH[1,*], D.P. SWANEY[2], R.W. BUDDEMEIER[3], M.R. SCARSBROOK[4], M.A. WEATHERHEAD[5], C. HUMBORG[6], H. ERIKSSON[7] and F. HANNERZ[8]

*[1]Centro de Investigación Científica y de Educación Superior de Ensenada (CICESE), Departamento de Ecología, Ensenada, Baja California, Mexico; [2]Boyce Thompson Institute, Cornell University, Ithaca, NY 14850, USA; [3]Kansas Geological Survey, University of Kansas, Lawrence, KS 66047, USA; [4]National Institute of Water and Atmospheric Research (NIWA), P.O. Box 11-115, Hamilton, New Zealand; [5]National Institute of Water and Atmospheric Research (NIWA), P.O. Box 8602, Riccarton, Christchurch, New Zealand; [6]Institute of Applied Environmental Research, Stockholm University, SE-10691 Stockholm, Sweden; [7]Department of Systems Ecology, Stockholm University, SE-10691 Stockholm, Sweden; [8]Department of Physical Geography, Stockholm University, SE-10691 Stockholm, Sweden; *Author for correspondence: Address: P.O. Box 434844, San Diego, CA 92143-4844, USA (e-mail: svsmith@cicese.mx; phone: +52-646-175-0500)*

Received 30 March 2004; accepted in revised form 10 November 2004

Key words: inorganic nutrient loading, population, runoff, catchment size, North America

Abstract. We have used a total of 496 sample sites to calibrate a simple regression model for calculating dissolved inorganic nutrient fluxes via runoff to the ocean. The regression uses the logarithms of runoff and human population as the independent variables and estimates the logarithms of dissolved inorganic nitrogen and phosphorus loading with R^2 values near 0.8. This predictive capability is about the same as has been derived for total nutrient loading with process-based models requiring more detailed information on independent variables. We conclude that population and runoff are robust proxies for the more detailed application, landscape modification, and in-stream processing estimated by more process-based models.The regression model has then been applied to a demonstration data set of 1353 river catchments draining to the sea from the North American continent south of the Canadian border. The geographic extents of these basins were extracted from a 1-km digital elevation model for North America, and both runoff and population were estimated for each basin. Most of the basins (72% of the total) are smaller than 10^3 km^2, and both runoff and population density are higher and more variable among small basins than among larger ones.While total load to the ocean can probably be adequately estimated from large systems only, analysis of the geographic distribution of nutrient loading requires consideration of the small basins, which can exhibit significant hydrologic and demographic heterogeneity between systems over their range even within the same geographic region. High-resolution regional and local analysis is necessary for environmental assessment and management.

Abbreviations BED – Baltic Environmental Database (Department of Systems Ecology, Stockholm University); DIN – dissolved inorganic nitrogen; DIP – dissolved inorganic phosphorus; IGBP – International Geosphere Biosphere Programme; LOICZ – Land Ocean Interactions in the Coastal Zone; N – nitrogen; NA – North American demonstration database; NAWQA – National Water Quality Assessment Program (United States Geological Survey); NRWQN – National River Water Quality Network (New Zealand National Institute of Water and Atmospheric Research); P – phosphorus; SPARROW – Spatially Referenced Regression on Watershed Attributes; TN – total nitrogen; TP – total phosphorus

Introduction

The cultural, or anthropogenic, eutrophication of coastal oceans as a result of the delivery of excess nutrients by rivers is a critical environmental issue on local, regional, and global scales (e.g. Rabalais et al. 2002). Understanding the global significance and estimating the magnitudes of fluvial nutrient delivery to the coastal ocean have been hampered both by lack of direct data on riverine nutrient fluxes, and by lack of generalizable predictive or correlative models that can relate nutrient delivery to more generally available data.

A recent study by Smith et al. (2003) analyzed river nutrient data assembled during the worldwide coastal zone nutrient budget development within the IGBP LOICZ project (http://data.ecology.su.se/MNODE/). The results of that study showed a significant relationship on the global scale between both basin population density and runoff per unit area. Peierls et al. (1991) and Caraco and Cole (1999) had previously used the data set assembled by Meybeck (1982) to argue that nitrate delivery to the world oceans is largely a function of population density, where that variable is both a driver in its own right and a proxy for other human variables such as land use, fertilizer application, and atmospheric nitrogen deposition. Lewis et al. (1999) and Lewis (2002) had also demonstrated a relationship with runoff in regional analyses. Smith et al. (2003), using a global data set containing numerous large and small basins, observed a significant relationship between nutrient fluxes and both runoff and population density.

Most large-scale regional or global analyses have relied heavily on data sets that can ultimately be traced back to Meybeck (1982), and involve a rather small number of rivers (28, for systems including both dissolved inorganic nitrogen and phosphorus; fewer for organic and particulate nutrients). Further, most of the river drainage basins in the 'Meybeck rivers' database are larger than 10^4 km^2. In addition to this data set, Smith et al. (2003) used river inorganic nutrient delivery data for 136 other sites, including some systems $<10^2$ km^2 in catchment area.

In addition to analysis of measured nutrient loads, it should be possible to use modeled nutrient discharge to augment the data set available. Models such as SPARROW (Smith et al. 1997; Alexander et al. 2000; http://water.usgs.gov/nawqa/sparrow/) and 'mass-balance models' (e.g. Howarth et al. 1996) can provide very useful calibrations between known point and non-point nutrient applications to catchments and the discharge of nutrients from the catchments, but their use depends on extensive, high-resolution databases that are simply not available for most of the world's river basins. It also seems likely that those watershed processes which control fluxes may be scale-dependent, requiring either different models or different parameterizations to be used at large and small scales (see, for example, the discussion by Caraco et al. 2003, on possible size dependence of NO_3 fluxes).

Several regional studies have also addressed relationships between specific sources and processes within watersheds and nutrient fluxes from the

watersheds (e.g. Alexander et al. 2002; Boyer et al. 2002; Mayer et al. 2002 for major watersheds of the northeastern United States; Howarth et al. 1996, for regions draining to the North Atlantic Ocean). Essentially all of these studies and model applications have been conducted in regions in which relatively detailed data are available to characterize the nutrient inputs to the watersheds. With the exception of Howarth et al. (1996), these results are from a geographically limited suite of temperate-zone, developed-country drainage basins.

Based on GIS modeling of world elevation gridded to 0.5 ° latitude/longitude, small (first and second order) river catchment basins apparently numerically dominate most of the global coastline length (Vörösmarty et al. 2000). This grid-scale resolution is approximately 2500 km^2 at low latitudes; the authors express high confidence in the depiction of basins >25,000 km^2 (i.e. about 10 times the grid-scale resolution) and diminished confidence for smaller basins. In their analysis, the small basins account for >90% of the total number of basins draining to the sea, and have an average area of about 6000 km^2 globally (4000 for North America) While the small basins only account for about 24% of the global continental area draining to the sea (32% for North America), it can be argued that existing inventories of basin characteristics, and particularly flux estimates, under-represent these small features. We therefore consider the present work critical to development of a much-needed understanding of the spatial distribution of fluvial nutrient loads along the world's coastline.

Objectives

This paper has two primary objectives. The first objective is to reexamine the nutrient flux regression equations developed by Smith et al. (2003), using an extended data set that includes more small systems. In other words, what, if any, insight is gained in considering small basins both in the calibration of nutrient flux models and in the application of the models regionally? The second objective is to apply those equations to a statistical population of river drainage basins that approximates the size, hydrological, and demographic distribution of basins draining to the ocean along a large coastal region. The region chosen for this analysis is temperate and tropical North America.

In this paper, we test the hypothesis that small drainage basins differ significantly from larger basins with regard to predictors of nutrient yields and the resulting coastal loads, and we explore reasons for the differences. In doing this, we apply additional basin loading data, in order to extend and refine the predictive load relationships developed by Smith et al. (2003). We also compare the resulting improved coastal load estimates with earlier findings and with independent estimates based on the SPARROW model. Finally, we apply the predictive regression relationship to estimate the coastal distribution of loads for most of the North American continent.

Materials and methods

Nutrient flux analysis

Data used

We have utilized five sets of basin load data representing nutrient fluxes (Table 1). Two of the loading data sets, labeled here as 'Meybeck' and 'LOICZ,' are those used (and described) by Smith et al. (2003). Both of these are worldwide in geographic extent (Figure 1a). In order to evaluate the possible role of small river basins in more detail, we have relied on three regional data sets, one from the US, one from New Zealand, and one for drainages to the Baltic Sea (Figure 1b–d).

The US Geological Survey National Water Quality Assessment program (NAWQA) includes flow-weighted nutrient concentrations as well as runoff, population density and other characteristics of the catchments. New Zealand's National River Water Quality Network (NRWQN) was provided by the New Zealand National Institute of Water and Atmospheric Research. For these data, flow-weighted nutrient concentrations were available, as well as runoff. Basin population data were estimated as described below for the demonstration data. For the Baltic Environmental Database (BED; http://data.ecology.su.se/models/bed.htm), river loads (1970–2000) can be accessed by a tool (called NEST) that is a web-distributed information environment for decision support systems. The river data are originally from Stålnacke et al. (1999), providing a monthly data set on nutrient loads and water discharge, based on 110 sampling stations within the Baltic Sea catchment. For the period 1991–2000 this data set has been updated (also monthly data), except for the Finnish rivers, using nutrient and water discharge data obtained from various environmental agencies.

Figure 1a, c, and d shows the centroids for the Meybeck, LOICZ, NRWQN, and BED data sets, as calculated from ArcView basin shape files. Shape files were not available for the NAWQA sites, so Figure 1b represents the catchment gauging stations. At the scale of the map, this geographic distinction is minor for most of the NAWQA basins.

While the Meybeck and LOICZ loading estimates were restricted to drainages directly entering the sea, the additional sites include watersheds and

Table 1. Data sets used for nutrient loading analyses.

Data sets	Number of basins	Data source
Meybeck	28	Meybeck (1982); see also Smith et al. (2003)
LOICZ	136	Smith et al. (2003)
NAWQA	175	http://water.usgs.gov/nawqa/nutrients/datasets/nutconc2000/
NRWQN	77	Smith and Maasdam (1994) and Maasdam and Smith (1994)
BED	80	http://data.ecology.su.se/models/bed.htm

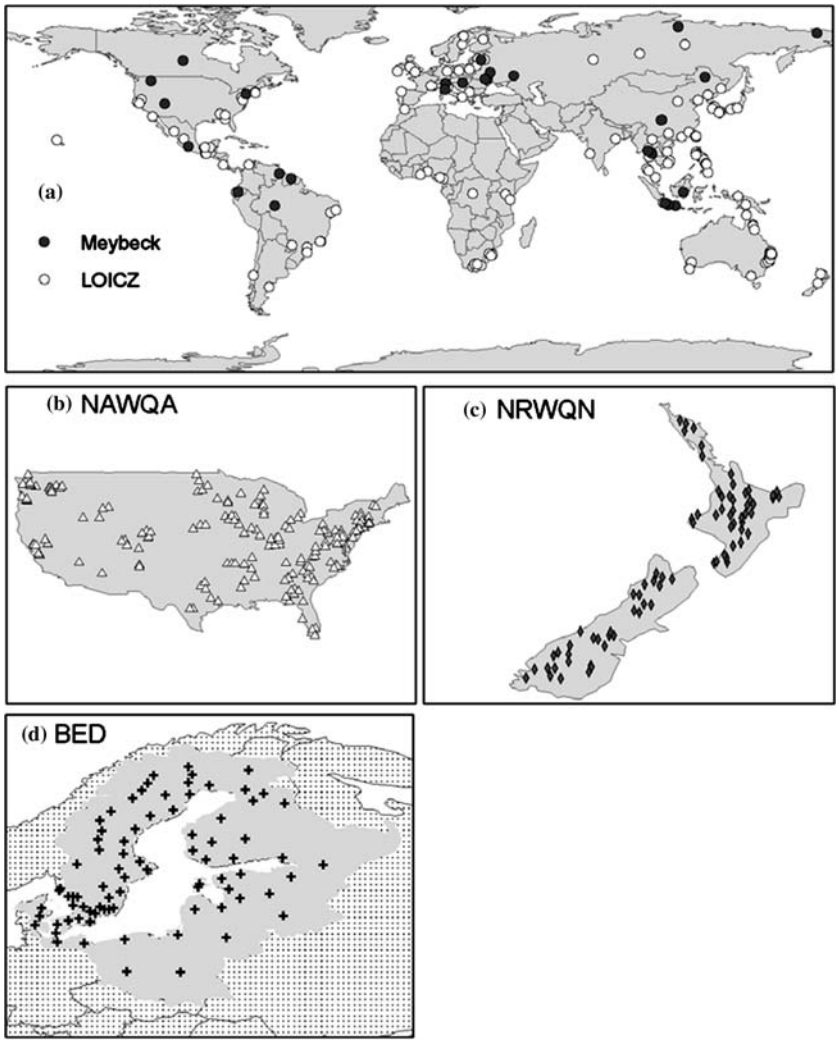

Figure 1. Sites used for calibrating the nutrient flux calculations. Basin geographical centers are plotted for panels (a), (c), and (d), while gauging station locations are plotted for (b).

sub-watersheds draining into larger downstream systems. Thus, the analysis not only expands the Smith et al. (2003) analysis and increases the number of smaller systems, but also extends the analysis to stream loads in general. A total of 496 sites have been used in the present recalibration of the response of DIN and DIP loading to runoff and population (Figure 1). This total is three times the number used for the original Smith et al. (2003) analysis.

Regression analysis and comparison data

The present analysis is an extension of the Smith et al. (2003) regression model for DIN and DIP yield (mol km^{-2} $year^{-1}$) as functions of population density (persons km^{-2}) and runoff per unit area (m $year^{-1}$). The methods and variables used are the same; however, in order to assess the variable of interest (nutrient load delivered to the coastal zone) more directly, the present paper analyzes the relationships in terms of basin load (mol $year^{-1}$), based on population (persons) and runoff (m^3 $year^{-1}$). Analyses included regression with the entire data set (presented here) and regressions with catchment size ranges within the data. We also used per cent error of load estimates (100 $\times$ (predicted $-$ observed load)/observed) to search for biases related to basin area, load, or yield in the load estimates.

The results of the load regressions developed are compared with the previous findings, with the results of regional assessments, and with the composite relationships developed from applications of the SPARROW model (Spatially Referenced Regression on Watershed Attributes) (Smith et al. 1997).

Analysis of spatial distribution of nutrient fluxes to the sea

An impetus behind this study was to estimate nutrient flux from the North American continent to the ocean. While nutrient flux data are available for many US rivers, few North American catchments south of the US border have been sampled. Therefore a second, 'demonstration' database was developed in order to examine the size distribution and hydrologic and demographic characteristics of North American watersheds draining to the ocean.

Only basins draining to the ocean and with their geographic centers south of the Canadian border were retained in this analysis. This minimizes effects that might be associated with catchments that are frozen for much of the year, and includes most North American catchments that have been significantly modified by human activities. Basin characteristics comparable to those used for the load data regressions were assembled for the demonstration database (NA) from three geospatially resolved, publicly available data sets using ArcView 3.2 and 8.3 (http://www.esri.com/), along with the Spatial Analyst extension for analysis of gridded data.

The first of these data sets was HYDRO1K digital elevation, runoff direction, and runoff accumulation data for North America (http://edcdaac.

Figure 2. Frequency distributions of areas for the global basin data used to calculate nutrient load regressions and predictions: (a) Meybeck; (b) LOICZ; (c) NAWQA; (d) NRWQN; (e) BED; (f) panels (a)–(d), combined; and (g) NA, the North American demonstration basins. The numbers in parentheses in the figure legends represent the number of basins in each data set. Smith et al. (2003) used (a) + (b) to calculate flux regressions; this paper uses the total (f), and applies the regressions to predicting loads based for NA (g).

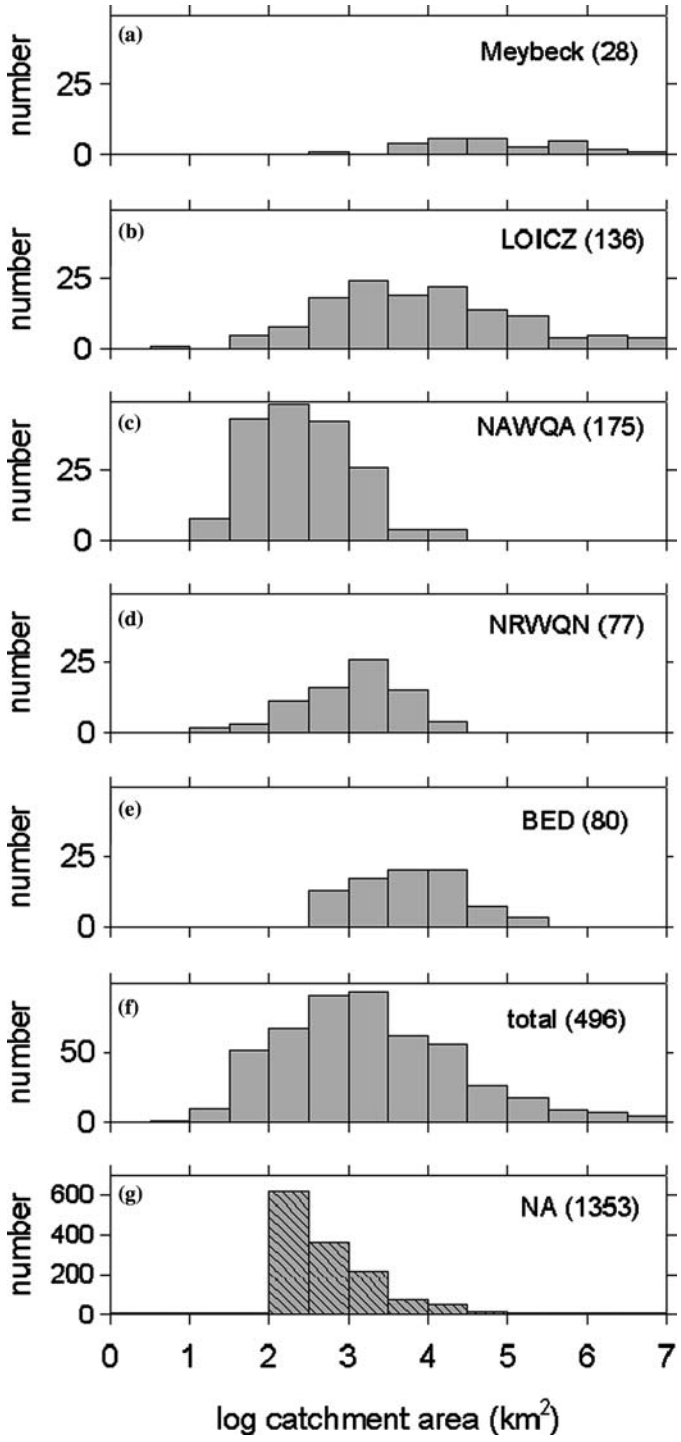
(a)
Meybeck (28)
(b)
LOICZ (136)
(c)
NAWQA (175)
(d)
NRWQN (77)
(e)
BED (80)
(f)
total (496)
(g)
NA (1353)
number
log catchment area (km^2)

usgs.gov/gtopo30/hydro/) (Verdin and Greenlee 1996). These data are resolved to a nominal grid scale of 1 km^2. We used these elevation data, with an ArcView 3 extension called 'Basin1,' in order to estimate the boundaries of watersheds for basins greater than or equal to 10^2 km^2 and draining to the ocean. This comprises the 'demonstration basin data set.' This procedure generated a total of 1353 basins along the coastline (Figure 2).

The second data set is Landscan population data for 2001 (Dobson et al. 2000; http://www.ornl.gov/gist/landscan/index.html) were used. These data are also resolved to a nominal grid scale of 1 km^2; the data were aggregated to the areas of the basins as outlined in step 1.

Finally, runoff is based on the Wilmott runoff surplus climatology (1950–2000) (monthly mean data, summed over the year; based on 150 mm rooting depth, resampled at 0.01° across the region of interest (http://climate.geog.udel.edu/~climate/). The monthly surplus across each basin (step 1) was accumulated over a year. Runoff surplus was adjusted upward by 1 mm $year^{-1}$ for every catchment, in order to avoid values of 0 in subsequent log transformations. Because the surplus is not corrected for water management (e.g. dams, or diversions) or groundwater flow, it represents estimated potential, rather than actual, runoff.

Estimates of runoff and population from steps 2 and 3, along with the loading equations developed in the loading analysis, were used to estimate nutrient loads for this demonstration basin data set. The nature of the analyses and databases used is such that, particularly for the smaller basins, the details of the calculated catchment boundaries, population densities, and runoff are uncertain. These uncertainties in the input data, in addition to the level of processing effort required, were the reasons for excluding basins $< 10^2$ km^2. However, we believe that this analysis represents an unbiased estimate of these features of the basins, and that the distribution shown in Figure 2g is a valid estimate of the actual basin size distributions. The locations and characteristics (basin size, population, runoff) of the North American basins used as the demonstration data set (NA) were analyzed and mapped, and are presented below.

Results

Basin sizes

Figure 2 shows the log-scale area distributions of the five individual loading data sets used in the calibration (2a–e), the combined total loading data set (2f), and the NA demonstration data set (2g). The Meybeck basins (2a) are relatively large in size and represent a small portion of the total. Addition of the LOICZ data set (2b) provides a significant number of smaller basins, but leaves the overall distribution skewed toward the large-basin end of the distribution. Further addition of the NAWQA, NRWQN, and BED data sets (2c–e) moves

the center of the size distribution towards substantially smaller systems. It appears (and is intuitively reasonable) that the loading basin data set still under-represents systems $<10^3$ km^2 in area.

This distribution of loading basin sizes can be compared with the NA demonstration basins. The demonstration data set is truncated at 10^2 km^2, for reasons of uncertain resolution of the basins and their characteristics at smaller sizes; if 'complete,' NA would contain a large number of smaller basins as well. Except for this truncation, the size distribution of the combined loading data set (2f) is more similar to the demonstration data set (2g) than to any of its constituent data sets.

Basin load regression equations

Figure 3 shows the regression plots for dissolved inorganic nitrogen and phosphorus (DIN, DIP), with the constituent data sets identified. Table 2 presents the regression equations derived from the 496 calibration basins described above, and for comparison, the results from Smith et al. (2003) and total nitrogen and total phosphorus (TN, TP) results from SPARROW Smith et al. 1997).

Note that the Smith et al. (2003) results are primarily discussed here as loading regressions, derived from the yield regressions originally developed in that paper. The modeled SPARROW results are for TN and TP, which we are comparing to the inorganic nutrient regressions, and are derived from a different, more extensive set of variables used in a georeferenced mechanistic model of nutrient application to the landscape and processed by landscape and in-stream processes. The SPARROW calibration data were from a geographically more restricted area (the US) than our global data. The only published

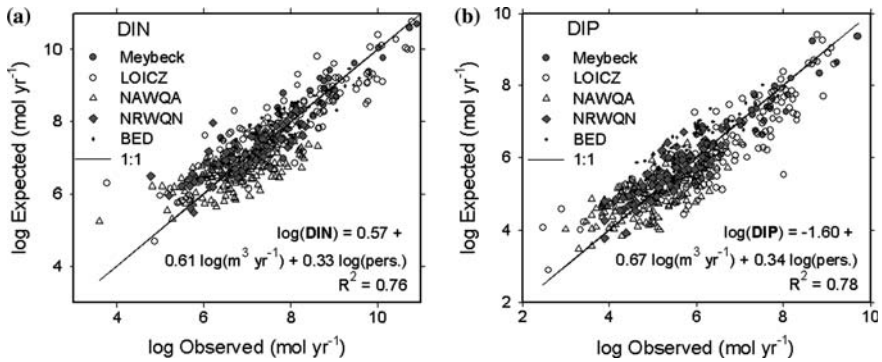

Figure 3. Scatter diagrams and regression equations for (a) DIN and (b) DIP loading (mol year^{-1}), for the 496 calibration basins.

Table 2. Regression analyses of N and P loading and yield.

Source	log N (mol $year^{-1}$)	R^2	log P (mol $year^{-1}$)	R^2
Loading equations				
Smith et al. (2003)	$-0.20 + 0.69 \times \log(run) + 0.32 \times \log(pers)$	0.81	$-1.15 + 0.66 \times \log(run) + 0.30 \times \log(pers)$	0.78
This paper	$0.57 + 0.61 \times \log(run) + 0.33 \times \log(pers)$	0.76	$-1.60 + 0.67 \times \log(run) + 0.34 \times \log(pers)$	0.78
SPARROW (Smith et al. 1997)		0.87		0.81
	log N (mol km^{-2} $year^{-1}$)	R^2	log P (mol km^{-2} $year^{-1}$)	R^2
Yield equations				
Smith et al. (2003)	$3.99 + 0.75 \times \log(run\ km^{-2}) + 0.35 \times \log(pers\ km^{-2})$	0.59	$2.72 + 0.78 \times \log(run\ km^{-2}) + 0.36 \times \log(pers\ km^{-2})$	0.58
This paper	$4.03 + 0.69 \times \log(run\ km^{-2}) + 0.36 \times \log(pers\ km^{-2})$	0.44	$2.43 + 0.63 \times \log(run\ km^{-2}) + 0.33 \times \log(pers\ km^{-2})$	0.38

In the cases of the results of Smith et al. (2003) and this paper, loading and regression are for dissolved inorganic N and P (DIN, DIP). For SPARROW, total N and P (TN, TP) loads are calculated. Correlations only are presented here for the SPARROW model loading estimates. (run = runoff (m^3/year); pers = number of persons).

values that can be used for direct comparison of the predictive capabilities of the SPARROW model and ours are the R^2 values.

It can be seen that R^2 for the two yield equations deteriorated, from about 0.6 in the Smith et al. (2003) paper to about 0.4 with the enlarged data set. The changes in the regression coefficients are not statistically significant ($p > 0.05$), suggesting that the additional data from generally smaller systems exhibit more variable yield. The loading equations did not change significantly, in either R^2 (about 0.8) or in the regression coefficients. Because the number of observations is much larger (496 vs. 164 sites), the confidence belts on the more recent regressions are tighter. The R^2 values for this rather simple loading model are relatively close to R^2 for TN loading according to the more elaborate (and data-intensive) SPARROW model and virtually identical to the value for TP according to that model.

Examination of the effect of basin size on the load and yield regression equations (Table 3) shows that the regression coefficients are remarkably constant, both across size scales and between the two nutrients. The differing intercepts for DIN and DIP, of course, arise because the DIN:DIP flux ratio is not unity, while the slope terms reflect the effects of the independent variables on the fluxes. These effects are very similar for this data set, suggesting that controls on N and P fluxes are closely related, at least statistically. Subsets of the data in different size classes produce similar results. The primary exception to these generalities about the coefficients is that a few of the coefficients for the smallest systems ($<10^2$ km^2) differ significantly from the other size classes. However, R^2 values for the small systems are substantially lower than they are for the larger systems, indicating that the regression models deteriorate for the smaller systems. The DIN load intercept for the largest systems ($>10^5$ km^2) differs from the overall intercept, implying that the extrapolation from very high loads to low loads is not good. This does not occur for DIP.

The structure of the R^2 values as functions of size is also interesting. The large systems ($>10^5$ km^2) tend to have higher values for R^2, with those values being close to (or above) the values for the total set of systems. The intermediate sizes of systems have somewhat lower R^2 values, and the systems $<10^2$ km^2 show substantially lower R^2 values.

Another way to evaluate the performance of the equations is to consider per cent error in the loading estimates ($100 \times$ [observed $-$ estimated]/observed), as functions of system size (Figure 4a and b). This analysis uses the overall regression equations, not the equations for each size of system. While there is no evident size-related bias in the errors, it can be seen that the error gets larger with small basins. This restates what was seen with the regressions partitioned by size. As seen for the overall equations, the mean loading errors for both DIN and DIP remain near 0 when evaluated with the equations for each range of basin size (Table 3).

Within the size range of the demonstration basins used later in this analysis (i.e. $>10^2$) km^2, our equations hold up well. Below that size, they are not good predictors, although neither the overall equations nor the size-partitioned

Table 3. Load and yield equations as a function of basin size.

Basin size (km^2)	Intercept	Runoff coeff.	Population coeff.	No. systems	R^2	Per cent load error
log DIN yield (mol km^{-2} $year^{-1}$)						
$<10^2$	4.32 ± 0.14	0.82 ± 0.23	0.20 ± 0.07	62	0.19	1.1 ± 1.3
10^2–10^3	4.09 ± 0.09	0.61 ± 0.10	0.38 ± 0.06	157	0.33	0.6 ± 0.8
10^3–10^4	3.97 ± 0.06	0.64 ± 0.08	0.38 ± 0.05	155	0.39	0.2 ± 0.6
10^4–10^5	3.79 ± 0.11	0.59 ± 0.09	0.38 ± 0.06	83	0.50	0.5 ± 0.7
$>10^5$	3.92 ± 0.40	0.89 ± 0.11	0.54 ± 0.09	39	0.79	0.0 ± 0.8
Total	4.03 ± 0.04	0.69 ± 0.05	0.36 ± 0.03	496	0.44	0.9 ± 0.4
log DIP yield (mol km^{-2} $year^{-1}$)						
$<10^2$	2.78 ± 0.15*	1.01 ± 0.25	0.14 ± 0.08*	62	0.19	1.1 ± 1.7
10^2–10^3	2.44 ± 0.08	0.63 ± 0.09	0.36 ± 0.05	157	0.37	1.9 ± 1.0
10^3–10^4	2.40 ± 0.07	0.68 ± 0.08	0.40 ± 0.05	155	0.40	0.5 ± 0.8
10^4–10^5	2.20 ± 0.14	0.48 ± 0.12	0.42 ± 0.08	83	0.37	1.3 ± 1.1
$>10^5$	2.44 ± 0.14	0.65 ± 0.09	0.39 ± 0.08	39	0.71	5.3 ± 0.8
Total	2.43 ± 0.04	0.63 ± 0.05	0.33 ± 0.03	496	0.38	1.5 ± 0.5
log DIN load (mol $year^{-1}$)						
$<10^2$	0.26 ± 1.35	0.71 ± 0.18	0.18 ± 0.06*	62	0.26	1.1 ± 1.3
10^2–10^3	0.26 ± 0.74	0.63 ± 0.09	0.38 ± 0.06	157	0.40	0.6 ± 0.8
10^3–10^4	1.02 ± 0.63	0.55 ± 0.07	0.34 ± 0.04	155	0.46	0.2 ± 0.6
10^4–10^5	0.24 ± 0.88	0.60 ± 0.09	0.39 ± 0.06	83	0.54	0.5 ± 0.7
$>10^5$	−0.76 ± 0.94*	0.67 ± 0.10	0.43 ± 0.10	39	0.76	0.0 ± 0.8
Total	0.57 ± 0.21	0.61 ± 0.03	0.33 ± 0.02	496	0.76	0.9 ± 0.4
log DIP load (mol $year^{-1}$)						
$<10^2$	−3.45 ± 1.49	1.00 ± 0.20	0.13 ± 0.07*	62	0.31	1.1 ± 1.7
10^2–10^3	−2.25 ± 0.68	0.73 ± 0.08	0.40 ± 0.05	157	0.49	1.9 ± 1.0
10^3–10^4	−1.22 ± 0.67	0.61 ± 0.0.07	0.37 ± 0.05	155	0.48	0.5 ± 0.8
10^4–10^5	−0.67 ± 1.12	0.52 ± 0.11	0.43 ± 0.08	83	0.41	1.3 ± 1.1
$>10^5$	−1.11 ± 0.73	0.61 ± 0.0.07	0.43 ± 0.08	39	0.81	5.3 ± 0.8
Total	−1.60 ± 0.22	0.67 ± 0.03	0.34 ± 0.02	496	0.78	1.5 ± 0.5

Value ± standard error. Values within basin-size categories marked with (*) are significantly different from the total data set at $p < 0.05$. The forms of the loading load and yield equations can be seen in Table 2.

equations appear to show any size-related trend in biases of the loading estimates. Presumably, controls on nutrient fluxes become more complex for the smaller systems, with more variability between systems. At large scales, that inter-system variability apparently is largely smoothed out, although the within-system heterogeneity is undoubtedly large. Thus, the equations we have explored perform relatively well down to systems $\sim 10^2$ km^2.

The distribution of observed data about the regression equations (Figure 3) suggests the possibility of a systematic deviation from the regression line at low loads. Figure 4c and d confirm this observation by examination of the per cent error in the predictions. Predicted DIN fluxes below 10^6 mol $year^{-1}$ and DIP fluxes below 10^4 mol $year^{-1}$ are biased above observed fluxes. In Figure 4e and f, it can also be seen that DIP yield is substantially overestimated at yields

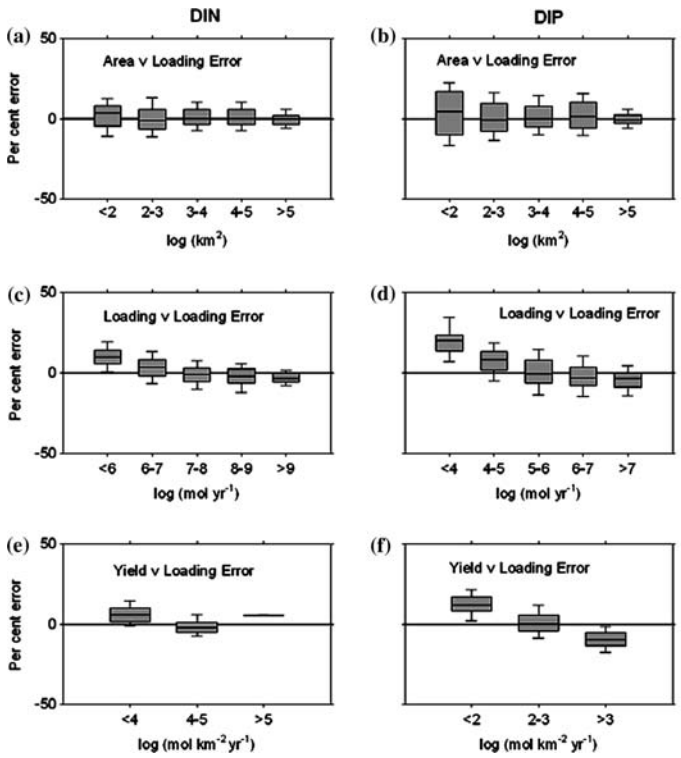

Figure 4. Box and whisker plots of area vs. nutrient loading error (a, b), loading vs. error (c, d), and yield vs. loading error (e, f) for the calibration basins. Each plot represents the median, 25th/75th percentiles, and 5th/95th percentiles with a black line within the box, the gray box itself, and whiskers above and below the box, respectively.

below 10^2 mol km^{-2} year^{-1} and underestimated at yields above 10^3 mol km^{-2} year^{-1}, while the equation for DIN yield should be relatively unbiased across the range of yields.

Demonstration basins

Distributions of the NA demonstration basin characteristics are shown in Figure 5 and Table 4. Although a total of 1353 basins greater than 10^2 km^2 in area were extracted for the region, basins between 10^2 and 10^4 km^2 in area are aggregated in the figure, because they are too small to be readily discerned on this figure at the continental scale. Basins that do not discharge to the sea and basins with centers outside the defined study area appear in white on the map. Shading on the map highlights the small basins (darker shades).

While the Mississippi River basin (diagonal hachure pattern) dominates the land area of the map ($\sim 3 \times 10^6$ km^2), most of the coastline length has basins

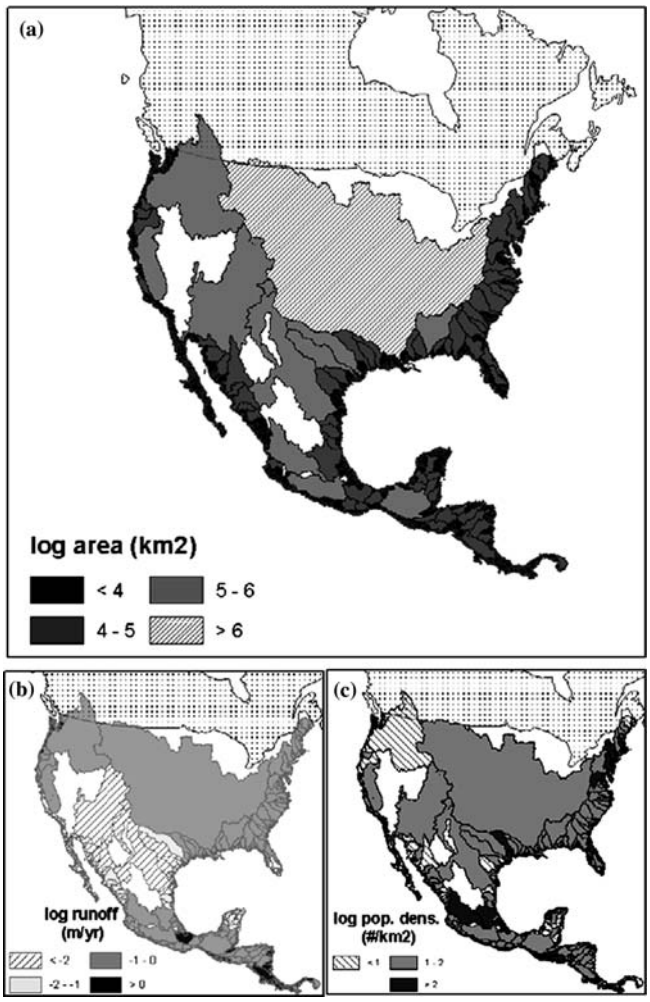

Figure 5. North American demonstration basins. These include temperate and tropical river basins $>10^2$ km^2 ($n = 1353$). (a) Shading is chosen to accentuate smaller catchments. White areas represent either internal drainages or outside the study area as defined in the text. (b, c) Runoff and population, both scaled to basin area. Dark shades accentuate strong contribution to nutrient flux.

$<10^4$ km^2 in area. There are 970 basins (72% of the total) $<10^3$ km^2 in area. Only 80 basins $>10^4$ km^2 are included in this analysis (6%). The coastline on Figure 5a is 'ragged' in appearance, because the map shows the basins, not the actual coastline. Thus, the ragged appearance reflects the existence of numerous coastal drainages $<10^2$ km^2 in area and excluded from this analysis (and from the map).

The inset maps (Figure 5b and c) show runoff (expressed in m year^{-1}) and population density (persons km^{-2}) for these basins. On these maps, darker shades indicate higher runoff and higher population density, and therefore

Table 4. Aggregate area, runoff, and population of the NA demonstration basins.

Area (km^2)	No. basins	Aggregate area (10^6 km^2)	Aggregate flow (10^9 m^3 $year^{-1}$)	Aggregate pop. (millions)	% of total area	% of total flow	% of total pop.	$\frac{\%\text{flow}}{\%\text{area}}$	$\frac{\%\text{pop.}}{\%\text{area}}$
10^2–10^3	970	0.32	170	29	3.7	8.0	8.5	2.2	2.3
10^3–10^4	303	0.82	394	57	9.4	18.4	16.7	2.0	1.8
10^4–10^5	69	1.70	635	109	19.4	29.7	32.0	1.5	1.6
10^5–10^6	10	2.72	407	74	31.1	19.0	21.7	0.6	0.7
$>10^6$	1	3.20	532	72	36.5	24.9	21.1	0.7	0.6
Total	1353	8.76	2138	341	100.0	100.0	100.0		

greater likely contribution to nutrient flux. The implications of the distributions of these variables are discussed below.

The calibration basins span a wider size range of runoff and population density than the demonstration basins. The low-size cutoff for the demonstration basins (10^2 km^2), evident in Figure 6a and b, is arbitrary, as described in the Methods; and the Mississippi basin is the only demonstration system $>10^6$ km^2 on those figures. In any case, it is desirable that the ranges of independent variables for the calibration systems equal or exceed that of the demonstration basins, in order to ensure that the regression equations are not extrapolated beyond the range of their data distributions. Except for a very small number of high-runoff systems and a somewhat larger number of low-runoff systems, that condition is met.

Both calibration sites and demonstration sites show a strong modal runoff equivalent to 0.1–1 m $year^{-1}$ of runoff (Figure 6a). The demonstration basins show a small secondary mode at 1 mm $year^{-1}$, below the values for most of the calibration sites. This mode is an artifact of adding 1 mm $year^{-1}$ to all basin runoff values in order to eliminate 0-runoff values. Population density (Figure 6b) is more variable for small basins, and the two data sets (calibration, demonstration) overlap. For both calibration and demonstration sites, the variability of population density decreases as system size increases, so inter-basin heterogeneity is smaller for large basins.

When runoff and population density are plotted against one another (Figure 6c), the calibration basins show a somewhat wider range of low population values and the demonstration basins appear to include more systems with low runoff. As already observed, the latter trend may represent the arbitrary assignment of 1 mm $year^{-1}$ to dry basins. In any case, the low population and low-runoff systems would represent low estimated loading rates. In general, we conclude that the overlap in these variables (area, runoff, population) is satisfactory for application of the regression equations to the demonstration sites.

It is also useful to examine the aggregate characteristics of the demonstration basins. The aggregate area of demonstration basins $<10^3$ km^2 is only about 13% of the total basin area, but both the flow:area ratio and the population:area ratio of these basins is about 2:1 (Table 4). Basins $>10^5$ km^2 account for 68% of

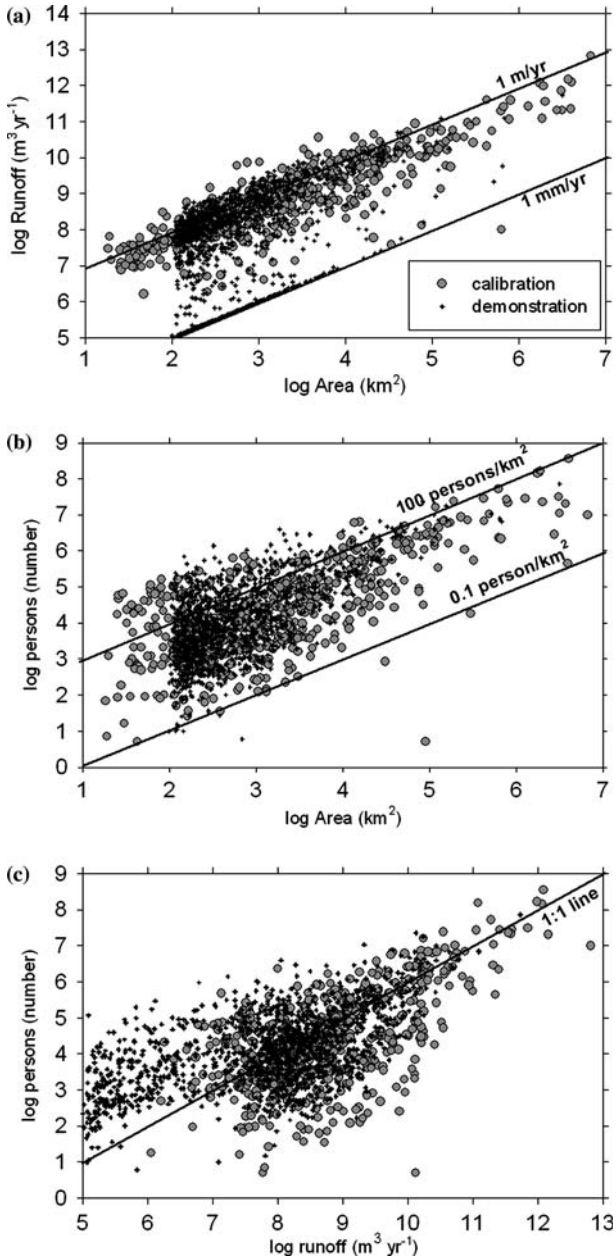

Figure 6. Comparison among area, runoff, and population density for the calibration sites and the demonstration sites. Trend lines added to aid in discussing the diagrams.

the total area, but have flow:area and population:area ratios well below 1:1. That is, the small basins show higher aggregate runoff and population density than the larger basins. The conclusion, from the scatter diagrams and the table of aggregate properties, is that the small demonstration basins show higher and more variable runoff and population density than the large basins.

Figure 6 demonstrates that the two data sets span similar ranges for the independent variables. This lends confidence to using the loading equations presented in Figure 3 and the demonstration basin characteristics shown in Figure 5 to estimate nutrient loads for the demonstration basins. It can be seen that the calculated loading for both DIN and DIP show a linear trend in log space, as illustrated by the diagonal lines on Figure 7a and b. It is not feasible to divide the demonstration data set into more than three categories due to the paucity of large basins. Relative load variability is much smaller for the largest basins than for the two smaller size classes. Comparatively few of the basins fall into the domain where loading would be seriously overestimated (i.e. below the dotted lines on the figures, as derived from inspection of Figure 4).

When the data are examined as a function of yield for the different size classes, a somewhat different pattern emerges (Figure 7c and d). The median yield across the size classes is virtually constant, and the variability of yield is much smaller in the largest basins than in the other two size classes, as was the

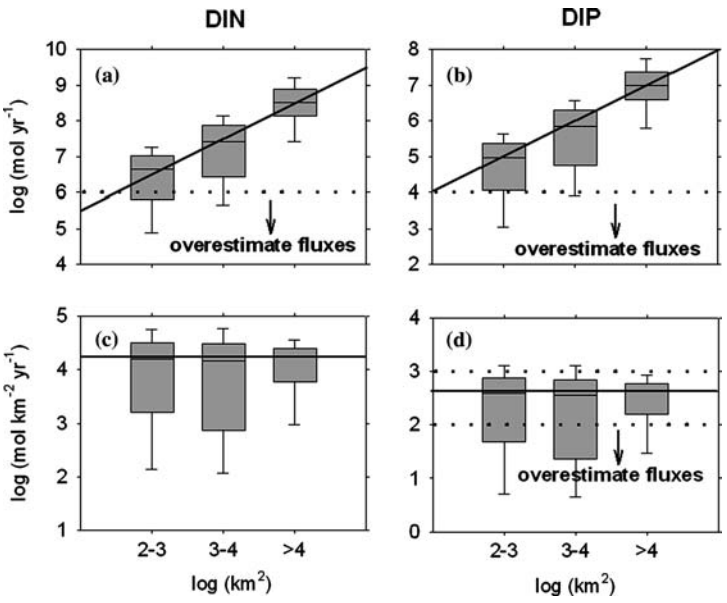

Figure 7. Box and whisker plots of estimated nutrient load (a, b) and yield (c, d) for the demonstration basins. Each plot represents the median, 25th/75th percentiles, and 5th/95th percentiles with a black line within the box, the gray box itself, and whiskers above and below the box, respectively. Also shown are extrapolation of the median load and yield for the large basins to other sizes (solid lines across the figures) and regions of model overestimates (and, in the case of DIP yield, underestimates), as derived from Figure 4.

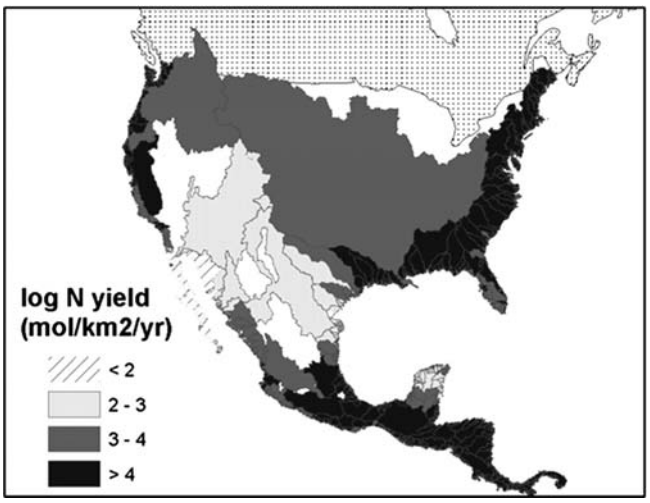

Figure 8. DIN yield as a function of basin size for the NA demonstration basins.

case with loads. We note that the most variable yields occur in the intermediate size class (i.e. basins between 10^3 and 10^4 km^2). While few of the high DIP yields would be underestimated for these basins, some (particularly within the intermediate-sized basins) would be overestimated.

Finally (Figure 8) we examine the spatial distribution of calculated fluxes for the demonstration basins, expressed as yields. Only DIN is presented, because the spatial pattern of DIP fluxes is qualitatively similar. The calculated fluxes for the NA demonstration basins are classed into four categories. As suggested by Figure 7c, some basins of all sizes are found to be in the intermediate yield categories. The most conspicuous areas of intermediate yield include the Mississippi basin (draining about half of the US) and various other large basins in the southwestern United States and Northern Mexico.

In contrast, high and low yields are largely confined to basins $< 10^4$ km^2. Very low yields are most common in northwestern Mexico, including the Baja California peninsula; this area is desert. Very high yields predominate along much of the Atlantic seaboard of the United States, as well as the isthmus of southern Mexico and Central America; there are also high-yield areas in the northwestern United States. All of these areas have high runoff and at least locally high population.

Discussion

Global analysis: estimated basin nitrogen loads

We have enlarged the Smith et al. (2003) database for small systems with US data from NAWQA, New Zealand data from NRWQN, and Baltic data from

BED. These represent the only readily available, relatively large databases of nutrient fluxes we have found to include many catchments $< 10^4$ km^2. The total nutrient flux database, while including many small systems, probably still under-represents smaller systems. Nevertheless the overlap in system characteristics between the loading data and the demonstration sites appears to be satisfactory (Figure 6). We hope that the results of the analysis presented here will encourage the development of a more extensive database for diverse, small river systems.

Figure 3 (observed vs. expected load for the loading calibration systems shown in Figure 1) demonstrates the large range in delivery, and Table 2 summarizes both the loading and yield equations. The R^2 for the nutrient loading equations are about 0.8, indicating that nutrient loading along the coastline should be rather well predicted by these simple relationships. This is borne out by regression analysis of the calibration data in five size classes and by analysis of the per cent error in load as a function of basin size (Figure 4).

Basin size: effects and implications

Caraco et al. (2003), in a paper provocatively asking 'Does one size fit all?' concluded that the overall simple loading model applied well across all scales, but that there seemed to be a slight bias for small basins. Small basins seemed, from their analysis, to be releasing a lower amount of NO_3 than larger basins as a result of either greater storage or higher gaseous N loss to the atmosphere. While the pattern may be true for some class of systems, our analysis (for total dissolved inorganic nitrogen) does not support this as an overall conclusion (Table 3 and Figure 4). We agree that there may be a size-related effect, but our interpretation for this effect differs from theirs.

Our suspicion is that any actual size-related trend may be hidden in the inter-basin heterogeneity that characterizes small and intermediate-sized systems. For example, the degree to which a basin denitrifies will be strongly controlled by land use (as both we and Caraco et al. recognize), and land use is likely to be more variable between small systems than between large systems. Their data set, particularly with respect to small systems, was from a relatively restricted range of climate types and vegetation. On average, their small systems were more heavily forested, and had higher runoff and lower population density than the larger systems. Agricultural activity, an activity known to be a major source of nutrients to the environment, is low in their small systems. Therefore the performance difference might reflect basin characteristics other than size. We do not see size-related error biases in our calibration data set, although the variability of flux increases with decreasing size (Figure 4a and b). We suggest that the explanation lies with inter-basin heterogeneity, rather than with size-dependent, within-basin performance differences.

Figure 6 shows log–log scatter plots of (a) basin area and runoff, (b) basin area and population, and (c) runoff and population, as estimated for both the

calibration and demonstration basins. The patterns for the two sets of basins are rather similar. The runoff distribution exhibits a central group of points and a secondary mode consisting of very dry basins (evident in the demonstration basins). Both high and low-runoff areas (Figure 6a) can be found over a wide range of basin sizes, and the points plot very close to the 1:1 line if only the relatively wet basins are considered. By contrast, population density is broadly unimodal, with a larger amount of scatter in small basin sizes than for larger sizes (Figure 6b).

Figure 6c combines the variables in a plot of population vs. runoff that brings into focus the characteristics discussed above, and helps to explain both the significance of the small basins and some of the results of this study. For basins of moderate to high total runoff and population – generally the larger basins – the points generally follow a 1:1 trend line. This means that either variable will be about as good as the other for explaining loads from the larger basins, and adding a second variable adds relatively little new information. This is consistent with the earlier studies that relied on the Meybeck data set and produced single-variable load dependencies (e.g. Peierls et al. 1991). At lower runoff values, the relationship beaks down. Therefore the two variables provide more information than either variable alone, and independent predictive abilities of each variable can be discerned.

Further consideration of Figure 6 suggests that the high inter-basin variability of both runoff and population density and the distinct low-runoff mode are major issues in these small basins. At sizes larger than about 10^4 km^2, the probabilities of extreme values in population, or little or no basin runoff, diminish. The fact that inter-basin variability is a major feature of small basins also helps to resolve the apparent paradox seen in Table 2 – expanding the number of data points and sampling a more nearly representative distribution results in decreases in the R^2 values for yield. This interpretation is confirmed by partitioning the calibration data into order-of-magnitude size classes and repeating the regression analyses (Table 3). The correlation coefficients are best for large systems that, although undoubtedly internally heterogeneous, are more similar between basins. For smaller basins, the correlations decrease, but the mean estimate of loading error remains near 0.

Finally, both the correlations and the regressions for either load or yield equations are most strongly affected for systems $< 10^2$ km^2. This suggests that, as the database expands, analysis of data subsets corresponding to various types of small basins may improve both predictive power and understanding of the observed relationships.

There seems likely to be some size below which size does matter, but perhaps not only for the reason given by Caraco et al. (2003). While small systems such as headwater streams can process DIN efficiently during periods of high biological activity (e.g. Peterson et al. 2001; Wollheim et al. 2001), we would argue that there is more inter-system variability in processes controlling flux from small systems related to variability in elevation, temperature, land-use history and other factors across small catchments (e.g. Ollinger et al. 1993; Murdoch

et al. 1998; Lawrence et al. 2000; Aber et al. 2003; Campbell et al. 2004). This is particularly well illustrated in the paper by Lovett et al. (2000) for NO_3 concentrations in small catchments of the Catskill Mountains of New York. A further point is that, particularly for small catchments, nutrient load may exceed the system assimilation capacity, especially following large precipitation or snowmelt events. (e.g. Rascher et al. 1987). Thus, for a particular load and as size diminishes, hydrological systems (including both their catchment and the stream itself) can eventually lose their capacity to retain that load.

Application and tests: the North America demonstration data

When the regression equations are applied to the demonstration basin data set, we find that for DIN, 50 basins (4% of the total number) account for about 75% of the load from temperate and tropical North America. The Mississippi alone accounts for about 25% (see also McIsaac et al. 2001). Based on these results, it is reasonable to assume that analyses of large river catchments probably provide an adequate characterization of total nutrient load to the ocean at the global or large regional scales. Simple upward scaling of large river nutrient fluxes to include all runoff should suffice to address that important global question. However, such analyses give little information on the geographic distribution of loads, and could be seriously misleading if used to infer biogeochemical and ecological performance of a coastal receiving water body in response to nutrient loading. Environmental assessment and management are local issues, and such analysis requires locally resolved loading estimates.

Regression models using independent variables which can be estimated from spatially explicit databases can meet the need for information about coastal nutrient loads at local and regional scale; we identify three classes of these models (see Alexander et al. 2002, for a more detailed discussion of model types and comparisons). The first of these classes assigns a mechanistic structure to the relationship among nutrient loads, landscape and in-stream nutrient processing, and lateral transfers. SPARROW (Spatially Referenced Regression on Watershed Attributes) (Smith et al. 1997; Alexander et al. 2000) has proven to be a remarkably successful application of this first class of models for the conterminous United States.

A second class of models assesses the relationship between one or more categories of nutrient inputs (atmospheric deposition, fertilizer, imported food/feed, etc.) to and nutrient fluxes from the watersheds in a somewhat more empirical fashion (Howarth et al. 1996, 2002; Seitzinger and Kroeze 1998; Boyer et al. 2002). These mass-balance models derive estimates of nutrient export as a fraction (typically $\sim$25%) of import. This class of models, too, has had a great deal of success for watersheds where data sets are available to adequately characterize the nutrient inputs, and in fact may yield predictions as good as or better than those derived from the first class of models (Alexander et al. 2002).

The third class of models compares loads to a minimal set of spatially distributed data (e.g. runoff, population) via regression analysis, without using an underlying mechanistic model structure or knowledge of the explicit forms of nutrient inputs or estimates of internal retention and relying instead on other variables as proxies. The model by Peierls et al. (1991), estimating nitrate yield from population density, was a seminal example of this class. The LOICZ regression model presented by Smith et al. (2003) and further calibrated here is another example of this latter class (see also Caraco and Cole 1999; Lewis et al. 1999; Lewis 2002).

The advantages of these regression models are twofold. First, they are computationally simple to apply on the basis of globally available high-resolution data, and second, they are applicable to the majority of the world's coastline, where the intensive data needed for the more explicitly mechanistic models are simply not available. These regression models are useful for assessing nutrient fluxes. Because the data entering these models are really serving as proxies for the actual drivers of nutrient flux, it should be recognized that such models have limited utility for nutrient management.

For example, about half of the coastline length represented by the North American analysis lacks the high-resolution data available for the United States which were used for the calibration of SPARROW or the mass-balance models. In most other regions, particularly in developing countries, the amount of high-resolution data available is much less than in the US. Seitzinger and Kroeze (1998) used nitrogen loading and related variables gridded to 1° of latitude and longitude (at low latitudes, an area of about 10^4 km^2). The most highly resolved global N loading estimates that we are aware of are those of van Drecht et al. (2001), nominally resolved at a scale of 0.5°. Almost 90% of the North American demonstration catchments examined here are smaller than the area of this latter resolution (i.e. <2500 km^2).

The simple model derived from LOICZ and refined here apparently predicts inorganic nutrient loads almost as well as the much more data-intensive SPARROW model predicts TN and TP loads, although the LOICZ model does not provide as much detailed insight into processes. Fertilizer use, animal agriculture wastes, and (for nitrogen) atmospheric deposition are the largest contributors of nutrients to the environment, and runoff is the major transport mechanism (discussed in many of the papers cited here). From the similar R^2 values for SPARROW and our model and the absence of size-related loading errors in our model, we infer that runoff and population are reasonably effective proxies for the landscape application, uptake, and routing terms in the SPARROW model or of the mass-balance models. Because runoff and population density can be estimated globally, for small areas, the regression model can be used to estimate the expected small-scale spatial variability of inorganic nutrient fluxes.

Summary and conclusions

Based on their numerical abundance and spatial dominance along much of the world coastline, small basins should be considered in order to develop either an adequate regression relationship or useful predictions of coastal zone characteristics and nutrient fluxes at local-to-regional scales. We have further tested and extended our earlier regression approach to coastal nutrient load prediction, using a substantially enlarged data set that includes more small basins. We have then explored the ramification of the nutrient flux relationships for basins draining to the coast from temperate and tropical North America.

Small and intermediate sized basins appear to behave differently, in terms of nutrient fluxes, than large basins. The major reason for this difference is interesting. Small basins contain heterogeneity between systems, while large systems contain heterogeneity within systems. Coefficients of regression equations describing nutrient fluxes do not shift significantly with the addition of small basins to the calibration database (at least down to scales of $\sim 10^2$ km^2). For smaller basins, the change in the regressions is increased variability, rather than a change in the underlying equations. Therefore the difference is apparently not a direct result of size. Rather, within the class of small basins, the difference in performance is apparently the result of both higher and more variable values for the independent variables from one small basin to the next. While the statistical independent variables in our model have been runoff and population, we would anticipate similar heterogeneity of the factors that directly control these nutrient fluxes.

References

Aber J.D. et al. 2003. Inorganic N losses from a forested ecosystem in response to physical, chemical, biotic and climatic perturbations. Ecosystems 5: 648–658.

Alexander R.B., Johnes P.J., Boyer E.W. and Smith R.A. 2002. A comparison of models for estimating the riverine transport of nitrogen from large watersheds. Biogeochemistry 57/58: 295–339.

Alexander R.B. et al. 2000. Atmospheric nitrogen flux from the watersheds of major estuaries of the United States: an application of the SPARROW watershed model. In: Valigura R.A. et al. (eds), Nitrogen Loading in Coastal Water Bodies: An Atmospheric Perspective. American Geophysical Union, Washington, DC, pp. 119–170.

Boyer E.W., Goodale C.I., Jaworski N.A. and Howarth R.W. 2002. Anthropogenic nitrogen sources and relationships to riverine nitrogen export in the northeastern U.S.A. Biogeochemistry 57/58: 137–169.

Campbell J.L. et al. 2004. Input–output budgets of inorganic nitrogen for 24 forest watersheds in the northeastern United States: a review. Water, Air Soil Pollut. 151: 373–396.

Caraco N.F. and Cole J.J. 1999. Human impact on nitrate export: an analysis using major world rivers. Ambio 28a: 167–170.

Caraco N.F., Cole J.J., Likens G.E., Lovett G.M. and Weathers K.C. 2003. Variation in NO_3 export from flowing waters of vastly different sizes: Does one size fit all? Ecosystems 6: 344–352.

Dobson J.E., Bright E.A., Coleman P.R., Durfee R.C. and Worley B.A. 2000. A global population database for estimating population at risk. Photogramm. Eng. Remote Sens. 66: 849–858.

Howarth R.W., Sharpley A. and Walker D. 2002. Sources of nutrient pollution to coastal waters in the United States: implications for achieving coastal water quality goals. Estuaries 25: 656–676.

Howarth R.W. et al. 1996. Regional nitrogen budgets and riverine N and P fluxes for the drainages to the North Atlantic Ocean: natural and human influences. Biogeochemistry 35: 75–139.

Lawrence G.B., Lovett G.M. and Baevsky Y.Y. 2000. Atmospheric deposition and watershed nitrogen export along an elevational gradient in the Catskill Mountains, New York. Biogeochemistry 50: 21–43.

Lewis W.M. 2002. Yield of nitrogen from minimally disturbed watersheds of the United States. Biogeochemistry 57/58: 375–385.

Lewis W.M. Jr., Melack J.M., McDowell W.H., McClain M. and Richey J.E. 1999. Nitrogen yields from undisturbed watersheds in the Americas. Biogeochemistry 46: 149–162.

Lovett G.M., Weathers K.C. and Sobczak W.V. 2000. Nitrogen saturation and retention in forested watersheds of the Catskill Mountains, New York. Ecol. Appl. 10: 73–84.

Maasdam R. and Smith D.G. 1994. New Zealand's National River Quality Network: 2. Relationships between physico-chemical data and environmental factors. New Zealand J. Mar. Freshwater Res. 28: 37–54.

Mayer B. et al. 2002. Sources of nitrate in rivers draining sixteen watersheds in the northeastern U.S.: isotopic constraints. Biogeochemistry 57/58: 171–197.

McIsaac G.B., David M.B., Gertner G.Z. and Goosby D.A. 2001. Nitrate flux in the Mississippi. Nature 414: 166–167.

Meybeck M. 1982. Carbon, nitrogen and phosphorus transport by world rivers. Am. J. Sci. 282: 401–450.

Murdoch P.S., Burns D.A. and Lawrence G.B. 1998. Relation of climate change to the acidification of surface waters by nitrogen deposition. Environ. Sci. Technol. 32: 1642–1647.

Ollinger S.V. et al. 1993. A spatial model of atmospheric deposition for the northeastern U.S. Ecol. Appl. 3: 459–472.

Peierls B., Caraco N., Pace M. and Cole J. 1991. Human influence on river nitrogen. Nature 350: 386–387.

Peterson B.J. et al. 2001. Control of nitrogen export from watersheds by headwater streams. Science 292: 86–90.

Rabalais N.N., Turner R.E. and Scavia D. 2002. Beyond science and into policy: Gulf of Mexico hypoxia and the Mississippi River. BioScience 52: 129–142.

Rascher C.M., Driscoll C.T. and Peters N.E. 1987. Concentration and flux of solutes from snow and forest floor during snowmelt in the West-Central Adirondack region of New York. Biogeochemistry 3: 209–224.

Seitzinger S.P. and Kroeze C. 1998. Global distribution of nitrous oxide production and N inputs in freshwater and coastal marine ecosystems. Global Biogeochem. Cycles 12: 93–113.

Smith D.G. and Maasdam R. 1994. New Zealand's National River Quality Network: 1. Design and physico-chemical characterisation. New Zealand J. Mar. Freshwater Res. 28: 19–35.

Smith R.A., Schwarz G.E. and Alexander R.B. 1997. Regional interpretation of water-quality monitoring data. Water Resour. Res. 33: 2781–2798.

Smith S.V. et al. 2003. Humans, hydrology, and the distribution of inorganic nutrient loading to the ocean. BioScience 53: 235–245.

Stålnacke P. et al. 1999. Estimation of riverine loads of nitrogen and phosphorus to the Baltic Sea, 1970–1993. Environ. Monit. Assess. 58(2): 173–200.

van Drecht G., Bouwman A.F., Knoop J.M., Meinardi C. and Beusen A. 2001. Global pollution of surface waters from point and nonpoint sources of nitrogen. The Scientific World 1(S2): 632–641.

Verdin K.L. and Greenlee S.K. 1996. Development of continental scale digital elevation models and extraction of hydrographic features. In: Proceedings, Third International Conference/ Workshop on Integrating. GIS and Environmental Modeling: 21–26 January 1996, Santa Fe, New Mexico.

Vörösmarty C.J., Fekete B.M., Meybeck M. and Lammers R.B. 2000. Global system of rivers: its role in organizing continental land mass and defining land-to-ocean linkages. Global Biogeochem. Cycles 14: 599–621.

Wollheim W.M. et al. 2001. Influence of stream size on ammonium and suspended particulate nitrogen processing. Limnol. Oceanogr. 46: 1–13.